ReaxFF User Manual

Written by Adri van Duin,
Original December 2002
Updated and expanded March 2013
Expanded June 2017 (e-ReaxFF)

Only relevant for the Standalone, single-processor, fortran-77 ReaxFF program, as written by Adri van Duin, 1999-2013, at the University of Newcastle upon Tyne (1999-2002), the California Institute of Technology (2002-2008) and the Pennsylvania State University (2008-2017)

E-mail: acv13@psu.edu
Department of Mechanical and Nuclear Engineering
Pennsylvania State University
University Park, PA 16802
USA

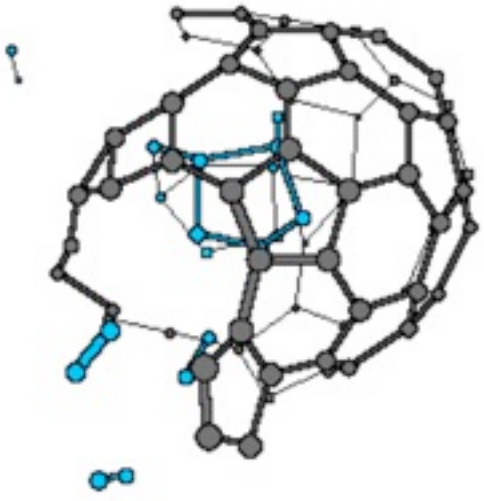

Contents

1. General overview

1.1 Concept. ReaxFF was developed to bridge the gap between quantum chemical (QC) and empirical force field (EFF) based computational chemical methods (Figure 1.1). Where QC methods are, in general, applicable to all chemical systems, regardless of connectivity, their computational expense makes them inapplicable for large (say, more than100 atoms) systems. Their computational expense also makes QC methods primarily applicable for single point or local energy minimization; high-temperature molecular dynamics (MD) simulations are generally too time-consuming.

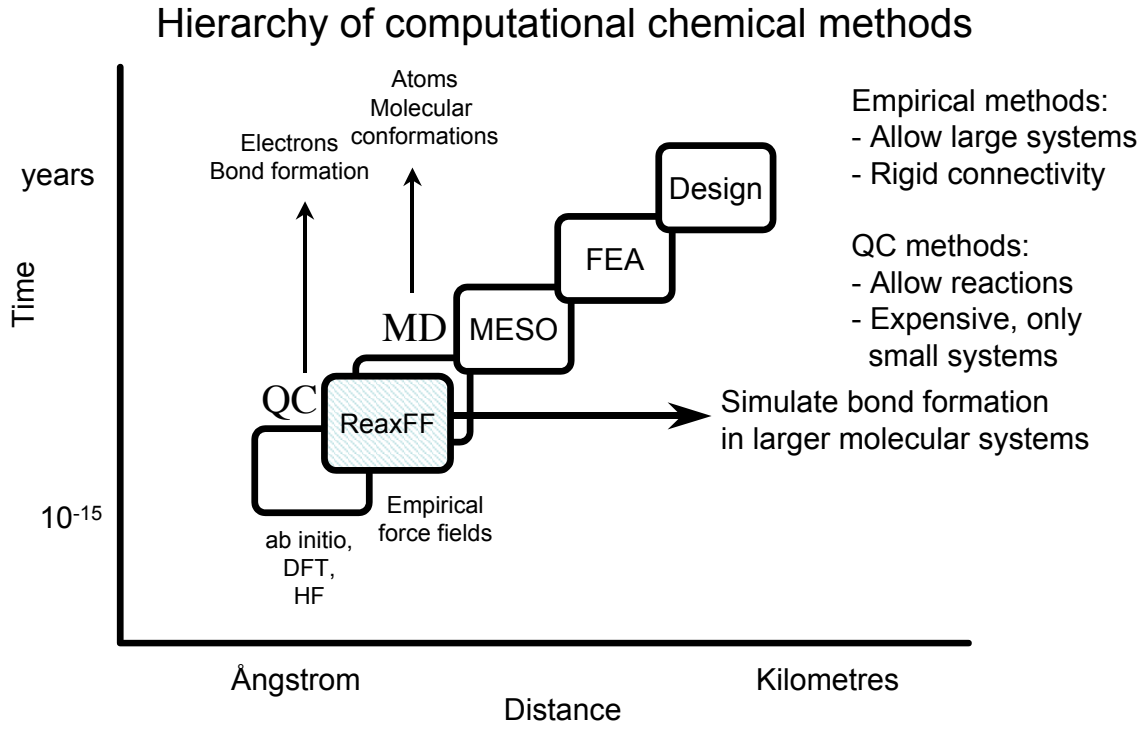

Figure 1.1: Position of ReaxFF in the computational chemical hierarchy.

EFF methods describe the relationship between energy and geometry with a set of relatively simple potential functions. In their most simple form, EFF methods describe molecular or condensed phase systems by simple harmonic equations that describe the stretching and compression of bonds and the bending of bond angles, usually augmented by van der Waals potential functions and Coulomb interactions to describe non-bonded interactions. Their relative simplicity allows EFF methods to be applied to much larger systems than QC systems (thousands of atoms on single processors; millions of atoms on multiprocessors). EFF methods have been very successful in describing physical interactions in and between molecules and condensed phase systems, and EFF methods haven been developed for a wide variety of chemical environments, including hydrocarbons, proteins and many inorganic systems. However, EFF methods are mainly applicable for systems at or around their equilibrium configuration. Due to their empirical nature, EFF methods require that the parameters used in their potential functions are

fitted against a suite of data, which can be gathered from experimental and/or from QC-sources (a.k.a. training set). The force field resulting from this fitting procedure can obviously be no more reliable than the data used in its training set. Furthermore, as the force field describes the system in an empirical rather than fundamental fashion, it should only be applied to systems similar to the ones present in the training set. As such, the quality and diversity of the training set define the transferability of the EFF method. With a few exceptions, current EFF methods are only trained for systems in which the bonds remain within about 75% of their equilibrium value. For this reason, these EFF methods cannot describe reactive systems, and in most cases the shape of the potential functions applied in these methods, like the aforementioned harmonic description of the bond length/bond energy relationship, would make it impossible to find parameter values that accurately describe bond energy towards the dissociation limit.

The concept of bond order/bond energy relation, as first formulated by Tersoff [lit], allows for the construction of EFF methods that can, in principle, handle connectivity changes. This concept was used by Brenner (Brenner, 1990) to construct the REBO-potential, an EFF method for hydrocarbon systems, allowing, for the first time, dynamical simulations of reactions in large (>>100 atoms) systems. Over the years, REBO has enjoyed widespread application, but its transferability is limited as it is based on a relatively small training set and because of its exclusion of all non-bonded interactions.

As with the Brenner potential, a bond order/bond energy relationship lies at the center of the ReaxFF-potential. Bond orders are obtained from interatomic distances (Figure 2) and are continually updated at every MD or energy minimization (MM) iteration, thus allowing for connectivity changes. These bond orders are incorporated in all valence terms (i.e. energy contributions dependent on connectivity, like valence angle and torsion angle energy) ensuring that energies and forces associated with these terms go to zero upon dissociation. Furthermore, ReaxFF describes non-bonded interactions between all atoms, irrespective of connectivity. Excessive short-range repulsive/attractive non-bonded interactions are circumvented by inclusion of a shielding term in the van der Waals and Coulomb interaction. For a more detailed description of the ReaxFF energy description see (van Duin et al., 2001) Chapter 4 of this manual and the recent ReaxFF review by Senftle et al. (Senftle et al., 2016).

Chapter 9 of this manual describes a recent extension of ReaxFF to include explicit electrons and holes (e-ReaxFF) – thus improving the ReaxFF capability to reproduce molecular electron affinities and ionization potentials – specifically enabling applications to reactions at electrochemical interfaces like batteries and fuel cells. This chapter specifically focuses on the practical simulation aspects associated with e-ReaxFF – input and output file structures. For a detailed description of the e-ReaxFF theory – and the affiliated ACKS2 charge calculation method – we refer to (Islam et al., 2016; Islam and van Duin, 2016) for e-ReaxFF and (Verstraelen et al., 2013) for the ACKS2-method charge calculation method.

ReaxFF aims to provide a transferable potential, applicable to a wide range of chemical environments. To ensure its transferability, the following general guidelines have been adopted in its development:

- No discontinuities in energy or forces, even during reactions.

- Each element is described by just one force field atom type. The ReaxFF metal oxide oxygen is described by the same parameters as the ReaxFF oxygen in organic molecules. ReaxFF does not have separate sp^2 and sp^3 atoms for carbon, the method determines the atoms hybridization from its chemical environment.
- No pre-definition of reactive sites is necessary using ReaxFF. Although it is possible to drive reactions using restraints (see Input files section) this is not required; given the right temperature and chemical environment reactions will happen automatically.

1.2 Features. At the moment of writing this manual, the ReaxFF-program supports the following features:

- NVT , NVE and NPT dynamics for molecular and periodic systems. Velocity and system volume scaling are performed using the Berendsen method. Velocity scaling can be performed on the entire system, on individual molecules or on individual atoms. Different temperature regimes can be applied to different parts of the system using the **tregime.in** file. This input file can also be used to increase and decrease system temperature during an MD-simulation and can be used to set op annealing runs. The **vregime.in**-file can be used to compress/expand and shear a periodic system.
- ReaxFF incorporates an external electric field. Using the **eregime.in**-file elaborate electric field regimes can be imposed on the system.
- Steepest descent, conjugate gradient and MD-based minimization methods.
- Numerical optimization of cell parameters. Default setting is for cubic optimization, but a/b/c parameters can be optimized separately. Also, c/a ratios can be varied separately (see sections on control and input geometry files). Also, low-temperature MD/NPT simulations can be used for cell parameter optimization.
- Numerical calculation of second derivatives. For molecular systems, these second derivatives can be used to calculate vibrational frequencies and modes. Using a harmonic approximation to populating these modes, ReaxFF can calculate entropy and related thermodynamic properties (see **thermo.out**-file).
- ReaxFF supports interatomic distance, angle, torsion angle and centre-of-mass restraints. These restraints can be used to drive reactions and can be defined in the **geo**-file (in .bgf-format). Sliding interatomic distance, angle and torsion restraints can be used in MD-simulations.
- ReaxFF can perform simulations on crystal unit cells, keeping track of bonds and valence angles between periodic images of atoms. Currently, this feature cannot be applied to systems requiring torsion angles across periodic boundaries (e.g. carbon crystals). None of the inorganic ReaxFF force fields developed to date have included torsion energy terms, and as such ReaxFF can do unit cell calculations for these systems. ReaxFF can also be used to create supercell structures (**fort.85**-output file).
- ReaxFF contains a force field optimization module. See input and output file sections for a further description.
- ReaxFF generates connection tables (see **fort.7** and **fort.8** output files) and performs a fragment analysis using a bond order cutoff (see **molfra.out**-file).
- Using the optional **addmol.bgf**-file, ReaxFF allows for the addition of a user-specified molecular fragment to the system at regular intervals. The initial position and velocity of this fragment can be fully defined by the user.

- ReaxFF has been developed around the EEM charge derivation method (Mortier et al., 1986), allowing calculation of geometry dependent charge distributions. As default, ReaxFF equilibrates the charges over the entire system, however, it can also equilibrate charges within each molecule or run with fixed charges (see **control**-file and **charges**-file in the input file section).
- ReaxFF generates. bgf, .geo, .xyz, .MOP, z-matrix (for molecules) and .pdf output files and can read .geo, .bgf, .xyz, .pdf and z-matrix files. Trajectories are saved in .xyz-format, with optional velocities. Restart files are generated at user-specified intervals.
- Optionally, ReaxFF can generate elaborate output on user-specified bond order/bond lengths and valency angles. See **control**-file, keyword ianalysis.

1.4 Current force fields. Figure 1.2 shows for which systems ReaxFF has currently been parameterized and at which stage of development these parameters sets are. Note that this figure only indicates the elements that have been visited by ReaxFF – it does not describe the actual materials. For example, while a ReaxFF description is available for Fe-metal and Fe/C/H/O interactions (Zou et al., 2012), we do not currently have parameters for the Fe/B or Fe/Si system available.

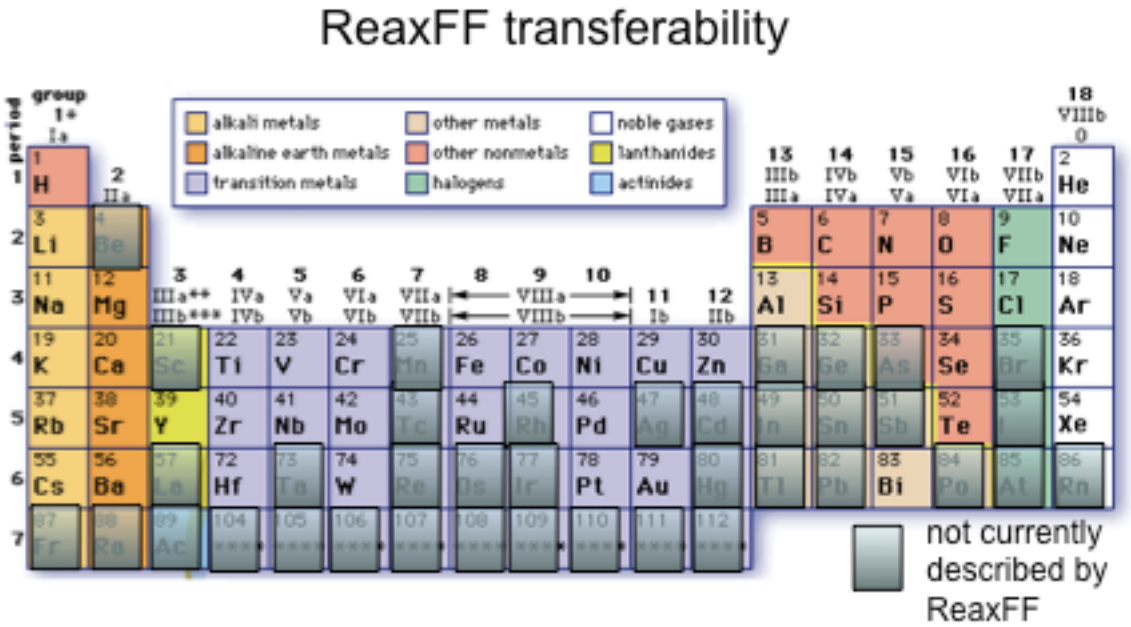

Figure 1.2. Overview of current elements supported by ReaxFF.

Training sets for these force fields primarily, and for many systems exclusively, consist of QC data on clusters and condensed phases. Although some of these reactive potentials have been applied successfully neither of these parameter sets are considered final. Our approach is that during an application we will continuously scrutinize the ReaxFF results by checking against QC data (probably by performing targeted QC-simulations on representative small systems). When major discrepancies occur the QC

data can be added to the appropriate training set and the parameters can be re-optimized. By this continuous communication between QC and ReaxFF we should obtain increasingly reliable and transferable reactive force field descriptions.

The currently available ReaxFF parameter sets have been mainly developed along two major development branch – the water-development branch and the combustion branch. Force field sharing a branch are fully transferable – they share general parameters and, for example, all contain the same first-row element (H/C/N/O) parameters. Figure 1.3 gives and overview of these development branches.

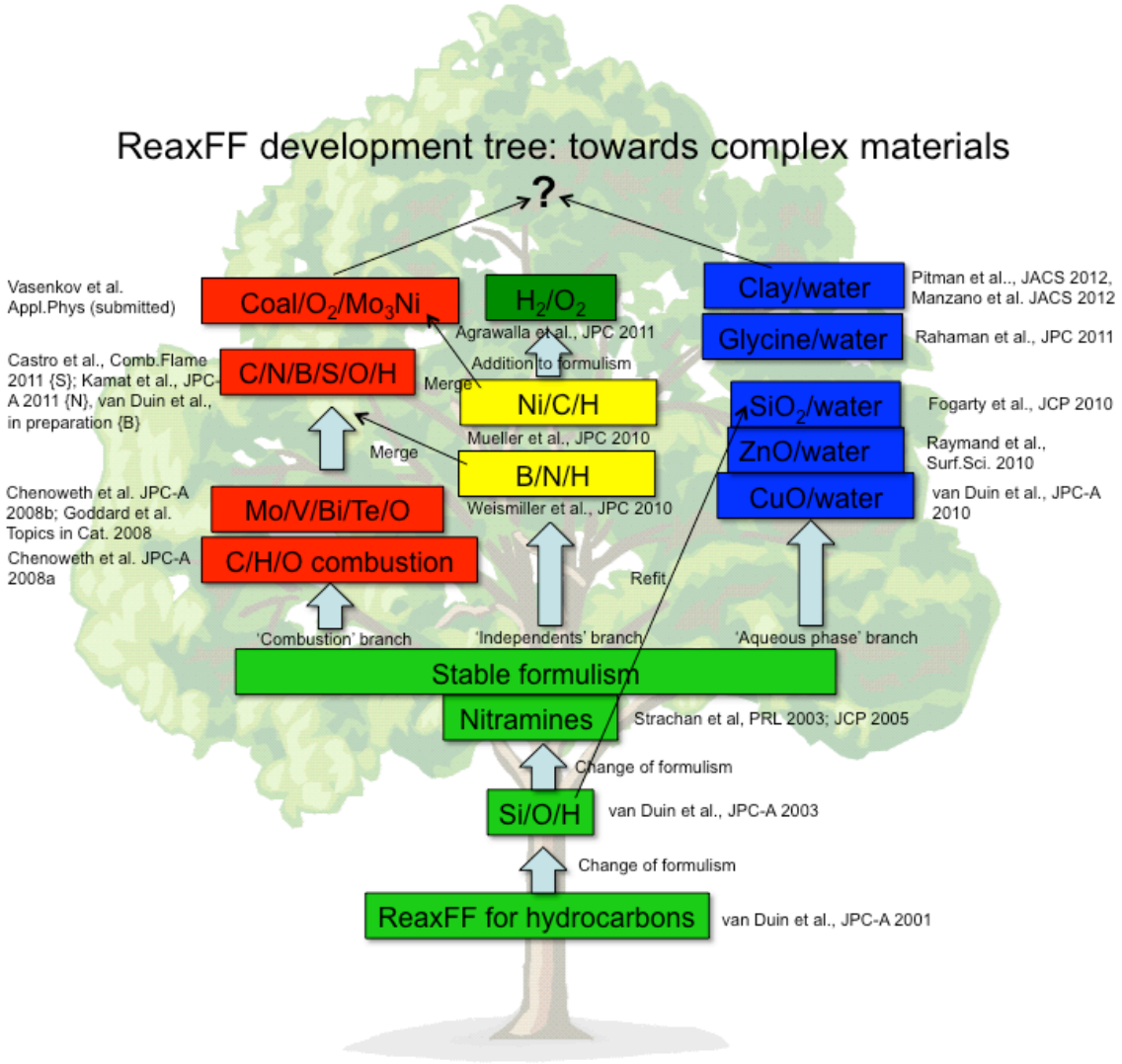

Figure 1.3 Historical overview of ReaxFF parameter development and transferability of published parameter sets on development branches.

Both of the two major development branches have been used for a wide range of materials – the water-branch contains a series of metal oxides, but also a protein and DNA description, while the combustion branch contains all first row elements, as well as a smaller number of oxides. The water-branch has been applied in the following publications: (Abolfath et al., 2011; Aryanpour et al., 2010; Bharati et al., 2012; Fogarty et al., 2010; Gale et al., 2011; Goken et al., 2011; Huang et al., 2013; Jeon et al., 2011; Jeon et al., 2012; Joshi and van Duin, 2013; Kim et al., 2012a; Kim et al., 2012b; Manzano et al., 2012a; Manzano et al., 2012b; Monti et al., 2013; Monti et al., 2012; Nomura et al., 2012; Pitman and van Duin, 2012; Rahaman et al., 2010; Rahaman et al., 2011; Raju et al., 2013; Raymand et al., 2011; Raymand et al., 2010; Russo et al., 2011; van Duin et al., 2010; van Duin et al., 2012; Vedadi et al., 2010; Yusupov et al., 2012).

The combustion branch has been used in the following publications:(Castro-Marcano et al., 2012; Chenoweth et al., 2009a; Chenoweth et al., 2008a, 2009b; Chenoweth et al., 2008b; Ganesh et al., 2011; Goddard et al., 2010; Jiang et al., 2009; Khalilov et al.,

2013a, b; Khalilov et al., 2012a; Khalilov et al., 2012b; Neyts et al., 2011; Salmon et al., 2009a, b; Srinivasan and van Duin, 2011). As Figure 1.3 indicates, there are also several 'Independent' force fields, not belonging to the two major development branches – however, most of these force fields have later been merged with the combustion branch. Several elements – like carbon, hydrogen, oxygen and silicon – are present on both the combustion and the water branch – once a training set is available we have found that it is fairly straightforward to transfer a parameter set from either the combustion branch to the water-branch, or vice versa. As such, we hope that in the future all these force fields can be combined into a single, fully transferable, ReaxFF description covering most of the periodic table.

4. Potential functions

This section contains all the general ReaxFF-potential functions. In the current ReaxFF code all the energy contributions in this document are calculated regardless of system composition. All parameters that do not bear a direct physical meaning are named after the partial energy contribution that they appear in. For example, p_{val1} and p_{val2} are parameters in the valence angle potential function. Parameters with a more direct physical meaning, like the torsional rotational barriers (V_1, V_2, V_3) bear their more recognizable names. These potential functions were published in (Chenoweth et al., 2008a)

1. Overall system energy

Equation (1) describes the ReaxFF overall system energy.

$$E_{system} = E_{bond} + E_{lp} + E_{over} + E_{under} + E_{val} + E_{pen} + E_{coa} + E_{C2} + E_{triple} + E_{tors} + E_{conj} + E_{H-bond} + E_{vdWaals} + E_{Coulomb} \quad (1)$$

Below follows a description of the partial energies introduced in equation (1).

2. Bond Order and Bond Energy

A fundamental assumption of ReaxFF is that the bond order BO'$_{ij}$ between a pair of atoms can be obtained directly from the interatomic distance r_{ij} as given in Equation (2). In calculating the bond orders, ReaxFF distinguishes between contributions from sigma bonds, pi-bonds and double pi bonds.

$$BO'_{ij} = BO'^{\sigma}_{ij} + BO'^{\pi}_{ij} + BO'^{\pi\pi}_{ij} = \exp\left[p_{bo1}\cdot\left(\frac{r_{ij}}{r_o^{\sigma}}\right)^{p_{bo2}}\right] + \exp\left[p_{bo3}\cdot\left(\frac{r_{ij}}{r_o^{\pi}}\right)^{p_{bo4}}\right] + \exp\left[p_{bo5}\cdot\left(\frac{r_{ij}}{r_o^{\pi\pi}}\right)^{p_{bo6}}\right] \quad (2)$$

Based on the uncorrected bond orders BO', derived from Equation 1, an uncorrected overcoordination Δ' can be defined for the atoms as the difference between the total bond order around the atom and the number of its bonding electrons *Val*.

$$\Delta'_i = -Val_i + \sum_{j=1}^{neighbour(i)} BO'_{ij} \quad (3a)$$

ReaxFF then uses these uncorrected overcoordination definitions to correct the bond orders BO'$_{ij}$ using the scheme described in Equations (4a-f). To soften the correction for atoms bearing lone electron pairs a second overcoordination definition Δ'^{boc} (equation 3b) is used in equations 4e and 4f. This allows atoms like nitrogen and oxygen, which bear lone electron pairs after filling their valence, to break up these electron pairs and involve them in bonding without obtaining a full bond order correction.

$$\Delta_i^{'boc} = -Val_i^{boc} + \sum_{j=1}^{neighbours(i)} BO_{ij}^{'} \quad (3b)$$

$$\begin{aligned} BO_{ij}^{\sigma} &= BO_{ij}^{'\sigma} \cdot f_1(\Delta_i^{'},\Delta_j^{'}) \cdot f_4(\Delta_i^{'},BO_{ij}^{'}) \cdot f_5(\Delta_j^{'},BO_{ij}^{'}) \\ BO_{ij}^{\pi} &= BO_{ij}^{'\pi} \cdot f_1(\Delta_i^{'},\Delta_j^{'}) \cdot f_1(\Delta_i^{'},\Delta_j^{'}) \cdot f_4(\Delta_i^{'},BO_{ij}^{'}) \cdot f_5(\Delta_j^{'},BO_{ij}^{'}) \\ BO_{ij}^{\pi\pi} &= BO_{ij}^{'\pi\pi} \cdot f_1(\Delta_i^{'},\Delta_j^{'}) \cdot f_1(\Delta_i^{'},\Delta_j^{'}) \cdot f_4(\Delta_i^{'},BO_{ij}^{'}) \cdot f_5(\Delta_j^{'},BO_{ij}^{'}) \\ BO_{ij} &= BO_{ij}^{\sigma} + BO_{ij}^{\pi} + BO_{ij}^{\pi\pi} \end{aligned} \quad (4a)$$

$$f_1(\Delta_i,\Delta_j) = \frac{1}{2} \cdot \left(\frac{Val_i + f_2(\Delta_i^{'},\Delta_j^{'})}{Val_i + f_2(\Delta_i^{'},\Delta_j^{'}) + f_3(\Delta_i^{'},\Delta_j^{'})} + \frac{Val_j + f_2(\Delta_i^{'},\Delta_j^{'})}{Val_j + f_2(\Delta_i^{'},\Delta_j^{'}) + f_3(\Delta_i^{'},\Delta_j^{'})} \right) \quad (4b)$$

$$f_2(\Delta_i^{'},\Delta_j^{'}) = \exp(-p_{boc1} \cdot \Delta_i^{'}) + \exp(-p_{boc1} \cdot \Delta_j^{'}) \quad (4c)$$

$$f_3(\Delta_i^{'},\Delta_j^{'}) = -\frac{1}{p_{boc2}} \cdot \ln\left\{ \frac{1}{2} \cdot \left[\exp\left(-p_{boc2} \cdot \Delta_i^{'}\right) + \exp\left(-p_{boc2} \cdot \Delta_j^{'}\right) \right] \right\} \quad (4d)$$

$$f_4(\Delta_i^{'},BO_{ij}^{'}) = \frac{1}{1 + \exp(-p_{boc3} \cdot (p_{boc4} \cdot BO_{ij}^{'} \cdot BO_{ij}^{'} - \Delta_i^{'boc}) + p_{boc5})} \quad (4e)$$

$$f_5(\Delta_j^{'},BO_{ij}^{'}) = \frac{1}{1 + \exp(-p_{boc3} \cdot (p_{boc4} \cdot BO_{ij}^{'} \cdot BO_{ij}^{'} - \Delta_j^{'boc}) + p_{boc5})} \quad (4f)$$

A corrected overcoordination Δ_i can be derived from the corrected bond orders using equation (5).

$$\Delta_i = -Val_i + \sum_{j=1}^{neighbours(i)} BO_{ij} \quad (5)$$

Equation (6) is used to calculate the bond energies from the corrected bond orders $BO_{ij.}$

$$E_{bond} = -D_e^{\sigma} \cdot BO_{ij}^{\sigma} \cdot \exp\left[p_{be1}\left(1 - \left(BO_{ij}^{\sigma}\right)^{p_{be2}}\right)\right] - D_e^{\pi} \cdot BO_{ij}^{\pi} - D_e^{\pi\pi} \cdot BO_{ij}^{\pi\pi} \quad (6)$$

3. Lone pair energy

Equation (8) is used to determine the number of lone pairs around an atom. Δ_i^e is determined in Equation (7) and describes the difference between the total number of outer shell electrons (6 for oxygen, 4 for silicon, 1 for hydrogen) and the sum of bond orders around an atomic center.

$$\Delta_i^e = -Val_i^e + \sum_{j=1}^{neighbours(i)} BO_{ij} \qquad (7)$$

$$n_{lp,i} = \mathrm{int}\left(\frac{\Delta_i^e}{2}\right) + \exp\left[-p_{lp1}\cdot\left(2 + \Delta_i^e - 2\cdot\mathrm{int}\left\{\frac{\Delta_i^e}{2}\right\}\right)^2\right] \qquad (8)$$

For oxygen with normal coordination (total bond order=2, Δ_i^e=4), equation (8) leads to 2 lone pairs. As the total bond order associated with a particular O starts to exceed 2, equation (8) causes a lone pair to gradually break up, causing a deviation Δ_i^{lp}, defined in equation (9), from the optimal number of lone pairs $n_{lp,opt}$ (e.g. 2 for oxygen, 0 for silicon and hydrogen).

$$\Delta_i^{lp} = n_{lp,opt} - n_{lp,i} \qquad (9)$$

This is accompanied by an energy penalty, as calculated by equation (10).

$$E_{lp} = \frac{p_{lp2}\cdot\Delta_i^{lp}}{1+\exp\left(-75\cdot\Delta_i^{lp}\right)} \qquad (10)$$

4. Overcoordination

For an overcoordinated atom (Δ_i>0), equations (11a-b) impose an energy penalty on the system. The degree of overcoordination Δ is decreased if the atom contains a broken-up lone electron pair. This is done by calculating a corrected overcoordination (equation 11b), taking the deviation from the optimal number of lone pairs, as calculated in equation (9), into account.

$$E_{over} = \frac{\sum_{j=1}^{nbond} p_{ovun1}\cdot D_e^\sigma \cdot BO_{ij}}{\Delta_i^{lpcorr} + Val_i}\cdot\Delta_i^{lpcorr}\cdot\left[\frac{1}{1+\exp\left(p_{ovun2}\cdot\Delta_i^{lpcorr}\right)}\right] \qquad (11a)$$

$$\Delta_i^{lpcorr} = \Delta_i - \frac{\Delta_i^{lp}}{1+p_{ovun3}\cdot\exp\left(p_{ovun4}\cdot\left\{\sum_{j=1}^{neighbours(i)}\left(\Delta_j - \Delta_j^{lp}\right)\cdot\left(BO_{ij}^{\pi} + BO_{ij}^{\pi\pi}\right)\right\}\right)} \qquad (11b)$$

5. Undercoordination

For an undercoordinated atom (Δ_i<0), we want to take into account the energy contribution for the resonance of the π-electron between attached under-coordinated atomic centers. This is done by equations 12 where E_{under} is only important if the bonds between under-coordinated atom *i* and its under-coordinated neighbors *j* partly have π-bond character.

$$E_{under} = -p_{ovun5} \cdot \frac{1-\exp\left(p_{ovun6} \cdot \Delta_i^{lpcor}\right)}{1+\exp(-p_{ovun2} \cdot \Delta_i^{lpcor})} \cdot \frac{1}{1+p_{ovun7} \cdot \exp\left[p_{ovun8} \cdot \left\{\sum_{j=1}^{neighbours(i)} \left(\Delta_j - \Delta_j^{lp}\right) \cdot \left(BO_{ij}^{\pi} + BO_{ij}^{\pi\pi}\right)\right\}\right]} \quad (12)$$

6. Valence Angle Terms

6.1 Angle energy. Just as for bond terms, it is important that the energy contribution from valence angle terms goes to zero as the bond orders in the valence angle goes to zero. Equations (13a-g) are used to calculate the valence angle energy contribution. The equilibrium angle Θ_o for Θ_{ijk} depends on the sum of π-bond orders (*SBO*) around the central atom *j* as described in Equation (13d). Thus, the equilibrium angle changes from around 109.47 for sp^3 hybridization (π-bond=0) to 120 for sp^2 (π-bond=1) to 180 for sp (π-bond=2) based on the geometry of the central atom j and its neighbors. In addition to including the effects of π-bonds on the central atom j, Equation (13d) also takes into account the effects of over- and under-coordination in central atom j, as determined by equation (13e), on the equilibrium valency angle, including the influence of a lone electron pair. Val^{angle} is the valency of the atom used in the valency and torsion angle evaluation. Val^{angle} is the same as Val^{boc} used in equation (3c) for non-metals. The functional form of Equation (13f) is designed to avoid singularities when *SBO*=0 and *SBO*=2. The angles in Equations (13a)-(13g) are in radians.

$$E_{val} = f_7(BO_{ij}) \cdot f_7(BO_{jk}) \cdot f_8(\Delta_j) \cdot \left\{p_{val1} - p_{val1} \exp\left[-p_{val2}\left(\Theta_o(BO) - \Theta_{ijk}\right)^2\right]\right\} \quad (13a)$$

$$f_7(BO_{ij}) = 1 - \exp\left(-p_{val3} \cdot BO_{ij}^{p_{val4}}\right) \quad (13b)$$

$$f_8(\Delta_j) = p_{val5} - (p_{val5} - 1) \cdot \frac{2+\exp\left(p_{val6} \cdot \Delta_j^{angle}\right)}{1+\exp\left(p_{val6} \cdot \Delta_j^{angle}\right)+\exp\left(-p_{val7} \cdot \Delta_j^{angle}\right)} \quad (13c)$$

$$SBO = \sum_{n=1}^{neighbors(j)} \left(BO_{jn}^{\pi} + BO_{jn}^{\pi\pi}\right) + \left[1 - \prod_{n=1}^{neighbours(j)} \exp\left(-BO_{jn}^{8}\right)\right] \cdot \left(-\Delta_j^{angle} - p_{val8} \cdot n_{lp,j}\right) \quad (13d)$$

$$\Delta_j^{angle} = -Val_j^{angle} + \sum_{n=1}^{neighbours(j)} BO_{jn} \quad (13e)$$

$$\begin{aligned} &SBO2 = 0 \text{ if } SBO \le 0 \\ &SBO2 = SBO^{p_{val9}} \text{ if } 0 < SBO < 1 \\ &SBO2 = 2 - (2 - SBO)^{p_{val9}} \text{ if } 1 < SBO < 2 \\ &SBO2 = 2 \text{ if } SBO > 2 \end{aligned} \quad (13f)$$

$$\Theta_o(BO) = \pi - \Theta_{0,0} \cdot \left\{1 - \exp\left[-p_{val10} \cdot (2 - SBO2)\right]\right\} \quad (13g)$$

6.2 Penalty energy. To reproduce the stability of systems with two double bonds sharing an atom in a valency angle, like allene, an additional energy penalty, as described in Equations (14a) and

(14b), is imposed for such systems. Equation (9b) deals with the effects of over/undercoordination in central atom *j* on the penalty energy.

$$E_{pen} = p_{pen1} \cdot f_9(\Delta_j) \cdot \exp\left[-p_{pen2} \cdot \left(BO_{ij} - 2\right)^2\right] \cdot \exp\left[-p_{pen2} \cdot \left(BO_{jk} - 2\right)^2\right] \quad (14a)$$

$$f_9(\Delta_j) = \frac{2 + \exp\left(-p_{pen3} \cdot \Delta_j\right)}{1 + \exp\left(-p_{pen3} \cdot \Delta_j\right) + \exp\left(p_{pen4} \cdot \Delta_j\right)} \quad (14b)$$

6.3 Three-body conjugation term. The hydrocarbon ReaxFF potential contained only a four-body conjugation term (see section 7.2), which was sufficient to describe most conjugated hydrocarbon systems. However, this term failed to describe the stability obtained from conjugation by the $–NO_2$-group. To describe the stability of such groups a three-body conjugation term is included (equation 15).

$$E_{coa} = p_{coa1} \cdot \frac{1}{1 + \exp\left(p_{coa2} \cdot \Delta_j^{val}\right)} \cdot \exp\left[-p_{coa3} \cdot \left(-BO_{ij} + \sum_{n=1}^{neighbours(i)} BO_{in}\right)^2\right] \cdot \exp\left[-p_{coa3} \cdot \left(-BO_{jk} + \sum_{n=1}^{neighbours(i)} BO_{kn}\right)^2\right] \cdot$$
$$\exp\left[-p_{coa4} \cdot \left(BO_{ij} - 1.5\right)^2\right] \cdot \exp\left[-p_{coa4} \cdot \left(BO_{jk} - 1.5\right)^2\right] \quad (15)$$

7. Torsion angle terms

7.1 Torsion rotation barriers. Just as with angle terms we need to ensure that dependence of the energy of torsion angle ω_{ijkl} accounts properly for BO $\rightarrow$ 0 and for BO greater than 1. This is done by Equations (16a)-(16c).

$$E_{tors} = f_{10}(BO_{ij}, BO_{jk}, BO_{kl}) \cdot \sin\Theta_{ijk} \cdot \sin\Theta_{jkl} \cdot$$
$$\left[\frac{1}{2}V_1 \cdot \left(1 + \cos\omega_{ijkl}\right) + \frac{1}{2}V_2 \cdot \exp\left\{p_{tor1} \cdot \left(BO_{jk}^{\pi} - 1 + f_{11}(\Delta_j, \Delta_k)\right)^2\right\} \cdot \left(1 - \cos 2\omega_{ijkl}\right) + \frac{1}{2}V_3 \cdot \left(1 + \cos 3\omega_{ijkl}\right)\right] \quad (16a)$$

$$f_{10}(BO_{ij}, BO_{jk}, BO_{kl}) = \left[1 - \exp\left(-p_{tor2} \cdot BO_{ij}\right)\right] \cdot \left[1 - \exp\left(-p_{tor2} \cdot BO_{jk}\right)\right] \cdot \left[1 - \exp\left(-p_{tor2} \cdot BO_{kl}\right)\right] \quad (16b)$$

$$f_{11}(\Delta_j, \Delta_k) = \frac{2 + \exp\left[-p_{tor3} \cdot \left(\Delta_j^{angle} + \Delta_k^{angle}\right)\right]}{1 + \exp\left[-p_{tor3} \cdot \left(\Delta_j^{angle} + \Delta_k^{angle}\right)\right] + \exp\left[p_{tor4} \cdot \left(\Delta_j^{angle} + \Delta_k^{angle}\right)\right]} \quad (16c)$$

7.2 Four body conjugation term. Equations (17a-b) describe the contribution of conjugation effects to the molecular energy. A maximum contribution of conjugation energy is obtained when successive bonds have bond order values of 1.5 as in benzene and other aromatics.

$$E_{conj} = f_{12}(BO_{ij}, BO_{jk}, BO_{kl}) \cdot p_{cot1} \cdot \left[1 + \left(\cos^2\omega_{ijkl} - 1\right) \cdot \sin\Theta_{ijk} \cdot \sin\Theta_{jkl}\right] \quad (17a)$$

$$f_{12}(BO_{ij}, BO_{jk}, BO_{kl}) = \exp\left[-p_{cot2} \cdot \left(BO_{ij} - 1\frac{1}{2}\right)^2\right] \cdot \exp\left[-p_{cot2} \cdot \left(BO_{jk} - 1\frac{1}{2}\right)^2\right] \cdot \exp\left[-p_{cot2} \cdot \left(BO_{kl} - 1\frac{1}{2}\right)^2\right] \quad (17b)$$

8. Hydrogen bond interactions

Equation (18) described the bond-order dependent hydrogen bond term for a X-H—Z system as incorporated in ReaxFF.

$$E_{Hbond} = p_{hb1} \cdot \left[1 - \exp\left(p_{hb2} \cdot BO_{XH}\right)\right] \cdot \exp\left[p_{hb3}\left(\frac{r_{hb}^{o}}{r_{HZ}} + \frac{r_{HZ}}{r_{hb}^{o}} - 2\right)\right] \cdot \sin^{8}\left(\frac{\Theta_{XHZ}}{2}\right) \quad (18)$$

9. Correction for C_2

ReaxFF erroneously predicts that two carbons in the C_2-molecule form a very strong (triple) bond, while in fact the triple bond would get de-stabilized by terminal radical electrons, and for that reason the carbon-carbon bond is not any stronger than a double bond. To capture the stability of C_2 we introduced a new partial energy contribution (E_{C2}). Equation (19) shows the potential function used to de-stabilize the C_2 molecule:

$$\begin{aligned} E_{C2} &= k_{c2} \cdot \left(BO_{ij} - \Delta_i - 0.04 \cdot \Delta_i^4 - 3\right)^2 \quad \text{if } BO_{ij} - \Delta_i - 0.04 \cdot \Delta_i^4 > 3 \\ E_{C2} &= 0 \qquad\qquad\qquad\qquad\qquad\quad \text{if } BO_{ij} - \Delta_i - 0.04 \cdot \Delta_i^4 \le 3 \end{aligned} \quad (19)$$

where Δ_i is the level of under/overcoordination on atom i as obtained from subtracting the valency of the atom (4 for carbon) from the sum of the bond orders around that atom and k_{c2} the force field parameter associated with this partial energy contribution.

11. Triple bond energy correction.

To describe the triple bond in carbon monoxide a triple bond stabilization energy is used, making CO both stable and inert. This energy term only affects C-O bonded pairs. Equation (20) shows the energy function used to describe the triple bond stabilization energy.

$$E_{trip} = p_{trip1} \exp\left[-p_{trip2}\left(BO_{ij} - 2.5\right)^2\right] \cdot \frac{\exp\left[-p_{trip4} \cdot \left(\sum_{k=1}^{neighbours(i)} BO_{ik} - BO_{ij}\right)\right] + \exp\left[-p_{trip4} \cdot \left(\sum_{k=1}^{neighbours(j)} BO_{jk} - BO_{ij}\right)\right]}{1 + 25 \cdot \exp\left[p_{trip3}\left(\Delta_i + \Delta_j\right)\right]}$$

12. Nonbonded interactions

In addition to valence interactions which depend on overlap, there are repulsive interactions at short interatomic distances due to Pauli principle orthogonalization and attraction energies at long distances due to dispersion. These interactions, comprised of van der Waals and Coulomb forces, are included for *all* atom pairs, thus avoiding awkward alterations in the energy description during bond dissociation.

12.1 Taper correction. To avoid energy discontinuities when charged species move in and out of the non-bonded cutoff radius ReaxFF employs a Taper correction, as developed by de Vos Burchart (1995). Each nonbonded energy and derivative is multiplied by a Taper-term, which is taken from a distance-dependent 7th order polynomial (equation 21)).

$$Tap = Tap_7 \cdot r_{ij}^7 + Tap_6 \cdot r_{ij}^6 + Tap_5 \cdot r_{ij}^5 + Tap_4 \cdot r_{ij}^4 + Tap_3 \cdot r_{ij}^3 + Tap_2 \cdot r_{ij}^2 + Tap_1 \cdot r_{ij} + Tap_0 \quad (21)$$

The terms in this polynomal are chosen to ensure that all 1st, 2nd and 3rd derivatives of the non-bonded interactions to the distance are continuous and go to zero at the cutoff boundary. To that end, the terms Tap_0 to Tap_7 in equation (21) are calculated by the scheme in equation (22), where R_{cut} is the non-bonded cutoff radius.

$$
\begin{aligned}
Tap_7 &= 20/R_{cut}^7 \\
Tap_6 &= -70/R_{cut}^6 \\
Tap_5 &= 84/R_{cut}^5 \\
Tap_4 &= -35/R_{cut}^4 \\
Tap_3 &= 0 \\
Tap_2 &= 0 \\
Tap_1 &= 0 \\
Tap_0 &= 1
\end{aligned}
\qquad (22)
$$

12.2 van der Waals interactions. To account for the van der Waals interactions we use a distance-corrected Morse-potential (Equations. 23a-b). By including a shielded interaction (Equation 23b) excessively high repulsions between bonded atoms (1-2 interactions) and atoms sharing a valence angle (1-3 interactions) are avoided.

$$
E_{vdWaals} = Tap \cdot D_{ij} \cdot \left\{ \exp\left[\alpha_{ij} \cdot \left(1 - \frac{f_{13}(r_{ij})}{r_{vdW}} \right) \right] - 2 \cdot \exp\left[\frac{1}{2} \cdot \alpha_{ij} \cdot \left(1 - \frac{f_{13}(r_{ij})}{r_{vdW}} \right) \right] \right\} \qquad (23a)
$$

$$
f_{13}(r_{ij}) = \left[r_{ij}^{p_{vdW}} + \left(\frac{1}{\gamma_w} \right)^{p_{vdW}} \right]^{\frac{1}{p_{vdW}}} \qquad (23b)
$$

12.3 Coulomb Interactions

As with the van der Waals-interactions, Coulomb interactions are taken into account between *all* atom pairs. To adjust for orbital overlap between atoms at close distances a shielded Coulomb-potential is used (Equation 24).

$$
E_{coulomb} = Tap \cdot C \cdot \frac{q_i \cdot q_j}{\left[r_{ij}^3 + \left(1/\gamma_{ij} \right)^3 \right]^{1/3}} \qquad (24)
$$

Atomic charges are calculated using the Electron Equilibration Method (EEM)-approach (Mortier et al., 1986). The EEM charge derivation method is similar to the QEq-scheme; the only differences, apart from parameter definitions, are that EEM does not use an iterative scheme for hydrogen charges (as in QEq) and that QEq uses a more rigorous Slater orbital approach to account for charge overlap.

5. Program structure

Figure 5.1 shows the general flow diagram of a typical molecular dynamics simulation using the ReaxFF code, which contains three main sections (ffopt.f, reac.f and poten.f). This flow diagram does not include the force field optimization section, which is essentially a shell written around the general ReaxFF code – this shell is predominantly located in the ffopt.f section.

For external codes aiming to link into the ReaxFF code – for example, a Monte Carlo external shell – the encalc subroutine is essentially at the core – this routine, which some minor initiation, can essentially be called as a force our energy library.

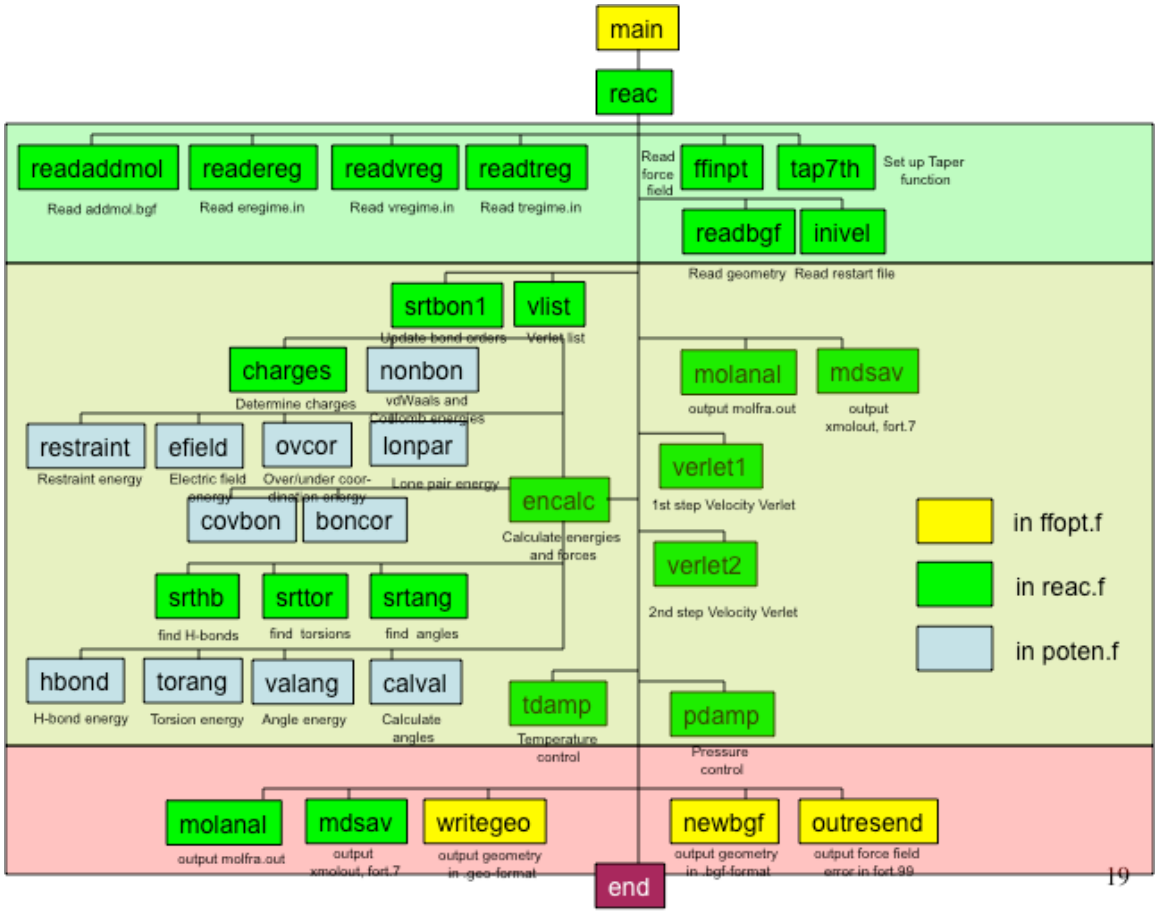

Figure 5.1. Flow diagram for a molecular dynamics simulation using the Standalone ReaxFF program.

6. Performance

Calculation speed for ReaxFF greatly depends on the atom connectivity. Slowest calculation speed is obtained for high-number density crystal systems requiring valence angle and torsion potentials (e.g. diamond). Furthermore, covalent materials that employ the bond order correction (Equations 3-4, Chapter 4), like carbon, are far more computationally demanding then materials that only use an uncorrected 2-body bond order (Equation 2, Chapter 4), like most metals.

Table 6.1 shows the ReaxFF calculation speed for some benchmark systems; these numbers are for the standalone code using a gnu-fortran 77-compiler without any optimization options. The Intel-compiler provides about 40% speed-up. To date, the largest system the standalone, non-parallel ReaxFF has been applied for contained about 5000 atoms. Ongoing developments in parallelizing the ReaxFF-code have greatly increase the feasible system size in parallel environments like LAMMPS and ADF (Aktulga et al., 2012; Shan et al., 2013; Zybin et al., 2010). Vashishta and co-workers have reported very large (>>1,000,000 parallel MD-simulations using their optimized USC/ReaxFF parallel code (Chen et al., 2010; Nakano et al., 2007; Nakano et al., 2008; Nomura et al., 2012; Nomura et al., 2007; Vashishta et al., 2006; Vedadi et al., 2010).

At low and medium temperatures (0-1500K) ReaxFF can run with time-steps of up to 0.25 femtoseconds and retain reasonable energy conservation. At higher temperatures smaller time-steps are required to retain energy conservation. This is also dependent on

Table 6.1: Benchmark runs for some crystal and molecular systems. Simulations were performed using NVE-molecular dynamics on a single-processor Dell T3600-workstation using a XEON E5-1620, 3.6 GHz processor with 16GB memory; EEM charges were updated every step. The Diamond crystal calculations involved valence and torsion angle energies, the Si(α) calculations did only involve valence angle energies.

System	#atoms	Time/MD iteration (s)
Diamond crystal	64	0.08
Diamond crystal	512	0.7
Si(α) crystal	64	0.012
Si(α) crystal	512	0.108
13 Methane molecules	65	0.022
104 Methane molecules	520	0.033
Fe-crystal	64	0.025
Fe-crystal	512	0.27

atom type – for systems with only heavy atoms (e.g. pure metal) larger time-steps may be feasible – this can be evaluated by performing an NVE-simulation at the temperature target; good energy conservation means that the selected time-step is acceptable.

7. Currently available execution environments

Besides the standalone ReaxFF program, which is described in this manual, there are a number of commercial and open-source codes available that contain a ReaxFF force engine. Most of these can read in the ReaxFF force field format, as described in this manual. We recommend that the energy output of any of these codes is first always compared to the standalone code – in case of discrepancy, the standalone code is always correct. Small energy deviations, for example due to different EEM-solvers used in parallel programs, are acceptable. Below follows a brief description of the execution environments that we are familiar with.

LAMMPS/ReaxFF. LAMMPS is an open-source, free, simulation environment that incorporates a large number of simulation methods, amongst which a ReaxFF force engine. LAMMPS also contains metadynamics tools – some of which can be used in conjunction with ReaxFF. LAMMPS enables massively parallel ReaxFF simulations (Shan et al., 2013; Zybin et al., 2010). The current ReaxFF implementation in LAMMPS is written in C++; this rewrite was performed by Metin Aktulga (Aktulga et al., 2012). We have used LAMMPS/ReaxFF for a number of systems – overall its integration runs very well, but we strongly recommend comparison between LAMMPS and standalone ReaxFF before running any large-scale simulations. LAMMPS can be downloaded from http://lammps.sandia.gov/.

ADF/ReaxFF. ADF is licensed by Scientific Computing & Modeling (SCM Amsterdam, the Netherlands, http://www.scm.com/). While originally focused on DFT calculations, recently SCM has integrated ReaxFF into ADF and is continuously expanding its functionality. The core of the ReaxFF engine in ADF is based on the standalone, fortran-77 code described here, which was re-mapped into a Fortran-95 environment to make the method more memory efficient; furthermore a significant optimization of the code was performed, making ADF/ReaxFF about 10 times faster than the standalone code described in this manual. ADF/ReaxFF also supports parallel molecular dynamics and incorporates various metadynamics tools.

Material Studio. Recently, Material Studio, licensed by Accelrys, started supporting ReaxFF, via the GULP module (http://accelrys.com/products/materials-studio/). This ReaxFF/GULP module was developed by Julian Gale – we believe this module to provide correct ReaxFF energies and forces, but recommend comparison with the standalone. At this moment, Material Studio only supports single-processor ReaxFF simulations.

Chapter 9. The e-ReaxFF method – inclusion of explicit electrons or holes

Introduction. As discussed in the previous sections of this manual, the ReaxFF method features a polarizable, geometry dependent charge calculation method – the EEM method. This enables ReaxFF to give a realistic description of the charge distribution within a molecular or condensed phase system. However – this charge calculation method is not accurate for the calculation of ionization potential and/or electron affinity – where the system fully accepts an electron or a hole. The main reason for this inaccuracy – which limits the reliability of the ReaxFF method for applications to electrochemically active interfaces, like batteries and fuel cells – is that the bond orders in ReaxFF are fully de-coupled from the charges – as such, a hydrogen atom that completely loses its electron through an ionization (H^+) is still considered capable of forming bonds. Similarly, a methane molecule in the ReaxFF description can be ionized and still retain a valency of 4 – thus creating a stable CH_4^+ radical cation. This is incorrect – the CH_4^+ radical cation only has 3 remaining valence electrons, and as such it should be unstable and form a CH_3^+ carbocation and a H-radical with zero or a small barrier. Similarly, ReaxFF predicts both H_2O and OH-radical to have positive electron affinities – i.e. both molecules can accept an additional electron forming, respectively, a H_2O^- radical anion and a OH^- anion. This is incorrect – while the OH-radical indeed has a strongly positive electron affinity, H_2O has a negative electron affinity, since the H_2O^- radical anion is highly unstable.
In order to remediate this incorrect description of electron affinity the ReaxFF concept was extended with the ability to describe explicit electrons or holes – this extension was named e-ReaxFF and is described in (Islam et al., 2016; Islam and van Duin, 2016). These electrons/holes carry a fixed -1/+1 charge. If these electrons or holes are captured by an atom then this results in a change in the number of valence electrons – following periodic table rules. For example – a carbon atom that capture a hole obtains an electron configuration of boron – which gives it a valency of 3. If the same carbon captures an electron it obtains a nitrogen electron configuration – giving it 5 valence electrons, of which 2 typically pair up as a lone pair, yielding an effective valency of 3 for the ReaxFF over- and undercoordination energy terms.

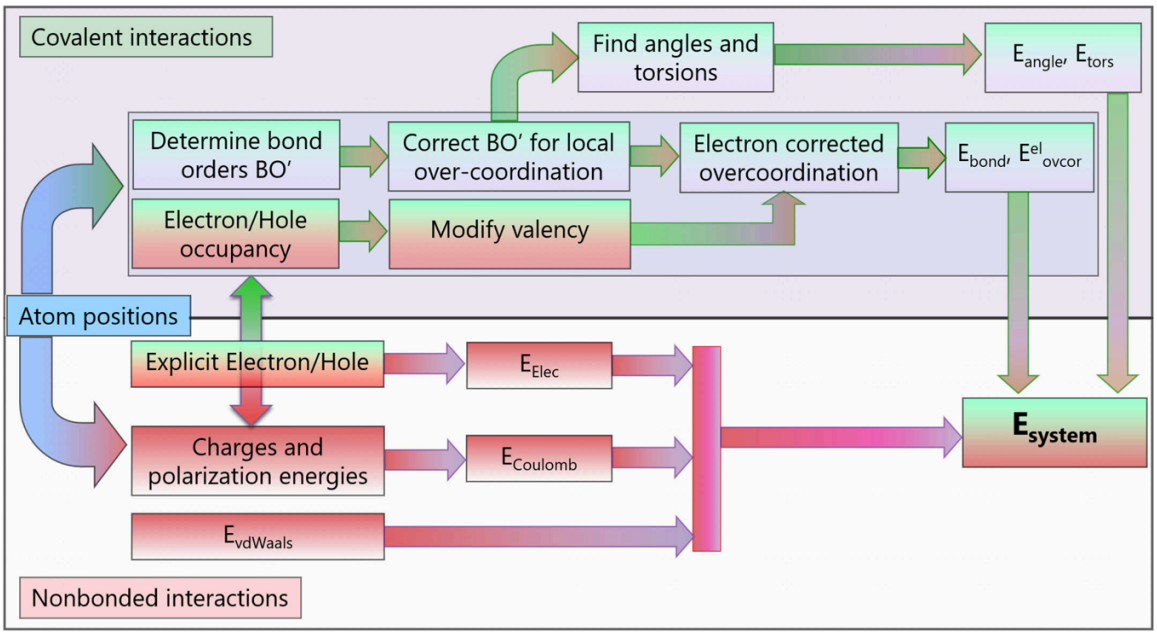

Figure 9.1; Schematic diagram indicating the e-ReaxFF concept.

Figure 9.1 schematically shows the e-ReaxFF concept. Note that, due to the fixed electron/hole charge, e-ReaxFF still keeps the bond-order based terms separate from the non-bonded terms – which is highly desirable from a computational expense perspective. As Figure 9.2 indicates – e-ReaxFF enables a far more accurate description of electron affinities for molecules – e-ReaxFF clearly identifies the low- or negative electron affinity for closed-shell molecules while recognizing the high electron affinity for radicals – see, in particular, the e-ReaxFF performance for methane, OH-radical and water.

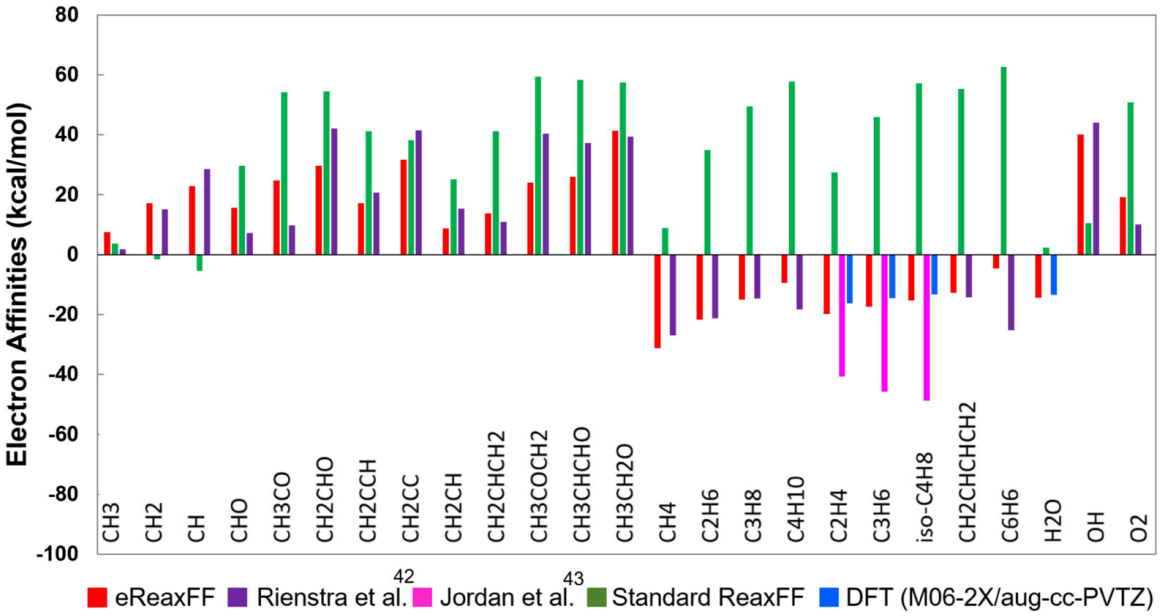

Figure 9.2 Comparison of ReaxFF and e-ReaxFF electron affinities to DFT-results.

It is important to note that in e-ReaxFF the electron/hole is essentially a particle – however, the electron/hole particle does not have to reside on a single atom – it can distribute itself over multiple atoms. In the current e-ReaxFF force fields, the mass of the electron/hole particles is 1 amu – this is mainly done to enable normal size MD-steps (typically 0.25 fs). The mass of the electron/hole particle can be straightforwardly modified in the force field file (see Example 2.8 and associated discussion). Furthermore, while e-ReaxFF can, in principle, work with EEM-charges, significant artificial charge transfer is typically observed when an explicit electron or hole is added to a molecule. EEM is not aware of chemical bond structure – as such, we often observe that a significant amount of the charge of a molecule/electron or molecule/hole pair is transferred to a neighboring molecule – which is physically suspect. As such, we recommend using the ACKS2 charge calculation – an extension of the EEM concept developed by Toon Verstraelen (Senftle et al., 2016; Verstraelen et al., 2013) instead of EEM. ACKS2 takes bonding structure into account during the charge calculation – resulting in effectively zero charge transfer between remote molecules. ACKS2 is currently supported in the standalone ReaxFF code and in ADF/ReaxFF.
e-ReaxFF is a relatively new method – and as such its capabilities and limitations are not yet fully established.

Equations Equations 9.1-9.3 describe the current e-ReaxFF formulation. These are straightforwardly added up to the normal ReaxFF equations.

In e-ReaxFF the electron/hole is described as a Gaussian wave (Equation 9.1)

$$\psi \infty exp(-\alpha(r-r')^2) \qquad (1)$$

This Gaussian wave interacts with the nuclei through a pairwise interaction, represented in Equation 9.2:

$$E_{nucl(i)-elec(j)} = -\frac{1}{4\pi\varepsilon_o}\beta \sum_{i,j} \frac{Z_i}{R_{ij}} erf\left(\sqrt{2\alpha}R_{ij}\right) \qquad (2)$$

Furthermore, the electron/hole carries a formal -1/+1 charge, which interacts with the other atomic charges through the regular ReaxFF shielded Coulomb interaction (Equation 8.24) which is also subject to the 7th order Taper function (Equation 8.22).

In addition to equations 9.2 and the Coulomb interaction, the electron/hole also affect the number of valence electrons of their neighboring atoms through Equation 9.3:

$$n_{el}=exp(-p_{val}*R_{ij}^2) \qquad (3)$$

This represents the amount of the hole/electron that belongs to a particular atom – note that this means that multiple atoms can own the electron/hole and can thus be affected. The number of valence electrons of an atom (Val_i equation 9.4) is subsequently modified by n_{el} from equation 9.3 using atom-specific rules (e.g. Carbon loses a valence electron both by hole/electron capture, Nitrogen loses a valence electron by electron capture but

gains a valence electron through hole capture) to get the amount of over/undercoordination Δ_i through equation 9.4.

$$\Delta_i = -\mathrm{Val}_i + \sum_{j=1}^{\mathrm{neighbor}(i)} \mathrm{BO}_{ij} \qquad (4)$$

Δ , derived from Equation 4, is subsequently modified to Δ_i^{xel} through a bond-type and atom-type dependent equation – resulting in an electron/hole corrected valence electron count for the atom (Equation 9.5) which subsequently enters the normal ReaxFF over/undercoordination terms (Equations 4.11a, 4.11b and 4.12)

$$\Delta_i^{\mathrm{xel}} = \Delta_i \cdot \exp\left(-p_i^{\mathrm{xel2}} \cdot n_{\mathrm{el}} \cdot \frac{\sum_{j=1}^{\mathrm{nbond}} \mathrm{BO}_{ij} \cdot p_{ij}^{\mathrm{xel1}}}{\sum_{j=1}^{\mathrm{neighbor}(i)} \mathrm{BO}_{ij}} \right) \qquad (5)$$

At this moment, only the under/overcoordination terms in ReaxFF are affected by the electron/hole modified valence electron count – the angle, dihedral and hydrogen bond terms still use the non-modified electron count.

Input/output files.
Geometry file. The explicit electrons and holes are added in the geo-file, as depicted in Example 9.1. Currently, the explicit electron is indicated by 'El' and the hole by 'Ho' – we acknowledge that the 'Ho' label can be confusing, as it might be mistaken for a Holbium atom (for which, currently, no ReaxFF parameters exist). The explicit charge of the electron or hole is set with MOLCHARGE keywords – note that it is required to also define the non-electron/hole atoms in MOLCHARGE keywords. We strongly recommend to put all the holes/electrons at the beginning or end of the geo-information, so that the rest of the non-electron/hole atoms can be captured in a single MOLCHARGE line and as such can freely exchange charges when molecular compositions change.

```
BIOGRF 200
DESCRP 08_w_el
REMARK w file created by Babel 1.6
MOLCHARGE   1   1 -1.00
MOLCHARGE   2  25  0.00
FORMAT ATOM   (a6,1x,i5,1x,a5,1x,a3,1x,a1,1x,a5,3f10.5,1x,a5,i3,i2,1x,f8.5)
HETATM     1 El                  39.99614  40.00419  40.00024    El  2 0  0.00000
HETATM     2 O                   39.11043  40.36875  37.76037    O   2 0  0.00000
HETATM     3 H                   38.54676  39.90381  38.44284    H   1 0  0.00000
HETATM     4 H                   39.98293  39.89636  37.88051    H   1 0  0.00000
HETATM     5 O                   41.51247  38.94035  38.32860    O   2 0  0.00000
HETATM     6 H                   41.73438  38.28709  37.66000    H   1 0  0.00000
HETATM     7 H                   41.05415  38.38735  39.04565    H   1 0  0.00000
HETATM     8 O                   39.75264  42.41341  39.51496    O   2 0  0.00000
HETATM     9 H                   39.27947  43.18404  39.19200    H   1 0  0.00000
HETATM    10 H                   39.51031  41.69227  38.83669    H   1 0  0.00000
HETATM    11 O                   37.70709  39.03190  39.85086    O   2 0  0.00000
HETATM    12 H                   37.96246  39.74552  40.53246    H   1 0  0.00000
HETATM    13 H                   36.75335  39.12421  39.78742    H   1 0  0.00000
HETATM    14 O                   42.28956  41.06839  40.27309    O   2 0  0.00000
HETATM    15 H                   42.17141  40.34847  39.61669    H   1 0  0.00000
HETATM    16 H                   41.51341  41.63285  40.06592    H   1 0  0.00000
HETATM    17 O                   40.21988  37.50300  40.35104    O   2 0  0.00000
HETATM    18 H                   40.52191  38.11673  41.05430    H   1 0  0.00000
HETATM    19 H                   39.33995  37.88268  40.14335    H   1 0  0.00000
HETATM    20 O                   38.50063  40.98387  41.64997    O   2 0  0.00000
HETATM    21 H                   38.87735  41.55897  40.92569    H   1 0  0.00000
HETATM    22 H                   39.31865  40.49040  41.94512    H   1 0  0.00000
HETATM    23 O                   40.94725  39.66444  42.28547    O   2 0  0.00000
HETATM    24 H                   41.45763  40.18520  41.57947    H   1 0  0.00000
HETATM    25 H                   41.33577  39.97570  43.10707    H   1 0  0.00000
FORMAT CONECT (a6,12i6)
UNIT ENERGY   kcal
ENERGY       -1923.014984
END
```

Example 9.1: Biograf input file for an 8-water, 1-explicit electron system. See Figure 9.3 for an image of this system.

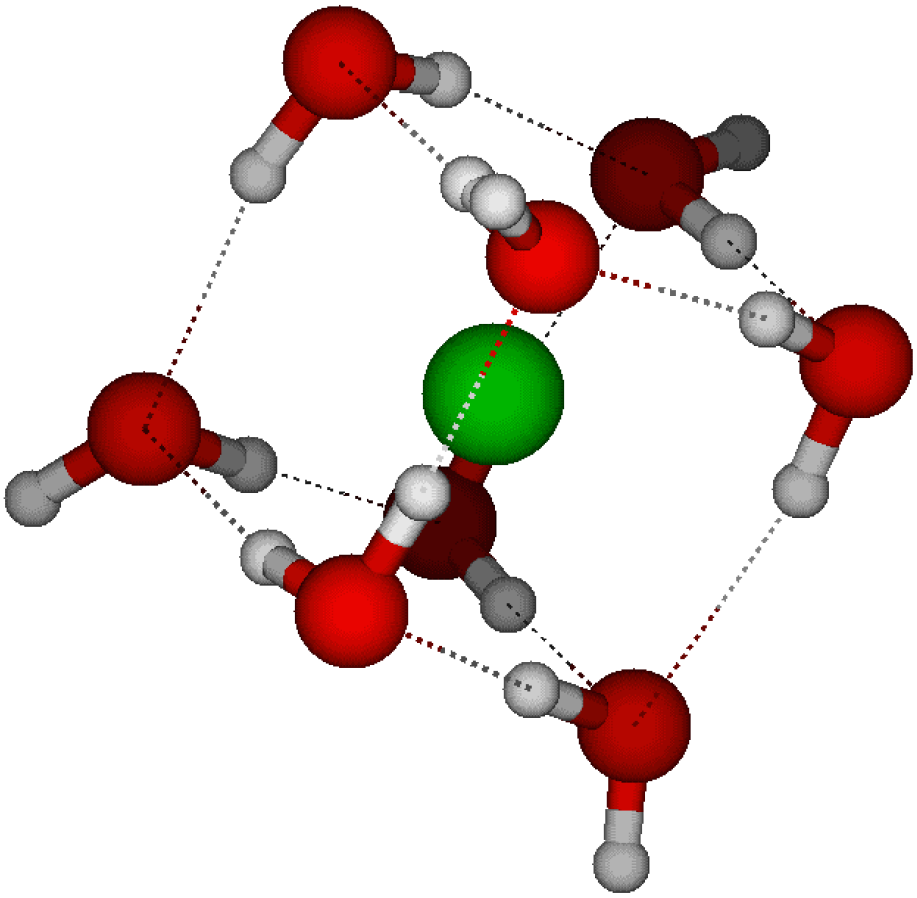

Figure 9.3. Structure of the 8-water, 1-electron system described in Example 9.1.

Note that for the visualization of the e-ReaxFF trajectories we typically change the ‘El’ atom type in the xmolout-trajectory to ‘Cl’ – since most visualization software can not handle the ‘El’ atom type.
When a second electron is added to the system from Example 9.1 and Figure 9.3 the input file will look like Example 9.2:

```
BIOGRF 200
DESCRP 8H2O_2el
MOLCHARGE   1   1 -1.00
MOLCHARGE   2   2 -1.00
MOLCHARGE   3  26  0.00
REMARK .bgf-file generated by xtob-script
HETATM     1 El                39.99614  40.00419  40.00024    Cl  0 0  0.00000
HETATM     2 El                38.04596  37.78193  36.99883    Cl  0 0  0.00000
HETATM     3 O                 39.11043  40.36875  37.76037    O   0 0  0.00000
HETATM     4 O                 38.50063  40.98387  41.64997    O   0 0  0.00000
HETATM     5 O                 39.75264  42.41341  39.51496    O   0 0  0.00000
HETATM     6 O                 37.70709  39.03190  39.85086    O   0 0  0.00000
HETATM     7 O                 41.51247  38.94035  38.32860    O   0 0  0.00000
HETATM     8 O                 40.94725  39.66444  42.28547    O   0 0  0.00000
HETATM     9 O                 40.21988  37.50300  40.35104    O   0 0  0.00000
HETATM    10 O                 42.28956  41.06839  40.27309    O   0 0  0.00000
HETATM    11 H                 38.54676  39.90381  38.44284    H   0 0  0.00000
HETATM    12 H                 39.98293  39.89636  37.88051    H   0 0  0.00000
HETATM    13 H                 41.73438  38.28709  37.66000    H   0 0  0.00000
HETATM    14 H                 41.05415  38.38735  39.04565    H   0 0  0.00000
HETATM    15 H                 39.27947  43.18404  39.19200    H   0 0  0.00000
HETATM    16 H                 39.51031  41.69227  38.83669    H   0 0  0.00000
HETATM    17 H                 37.96246  39.74552  40.53246    H   0 0  0.00000
HETATM    18 H                 36.75335  39.12421  39.78742    H   0 0  0.00000
HETATM    19 H                 42.17141  40.34847  39.61669    H   0 0  0.00000
HETATM    20 H                 41.51341  41.63285  40.06592    H   0 0  0.00000
HETATM    21 H                 40.52191  38.11673  41.05430    H   0 0  0.00000
HETATM    22 H                 39.33995  37.88268  40.14335    H   0 0  0.00000
HETATM    23 H                 38.87735  41.55897  40.92569    H   0 0  0.00000
HETATM    24 H                 39.31865  40.49040  41.94512    H   0 0  0.00000
HETATM    25 H                 41.45763  40.18520  41.57947    H   0 0  0.00000
HETATM    26 H                 41.33577  39.97570  43.10707    H   0 0  0.00000
END
```

Example 9.2: Biograf input file for an 8-water, 2-explicit electron system. See Figure 9.4 for an image of this system.

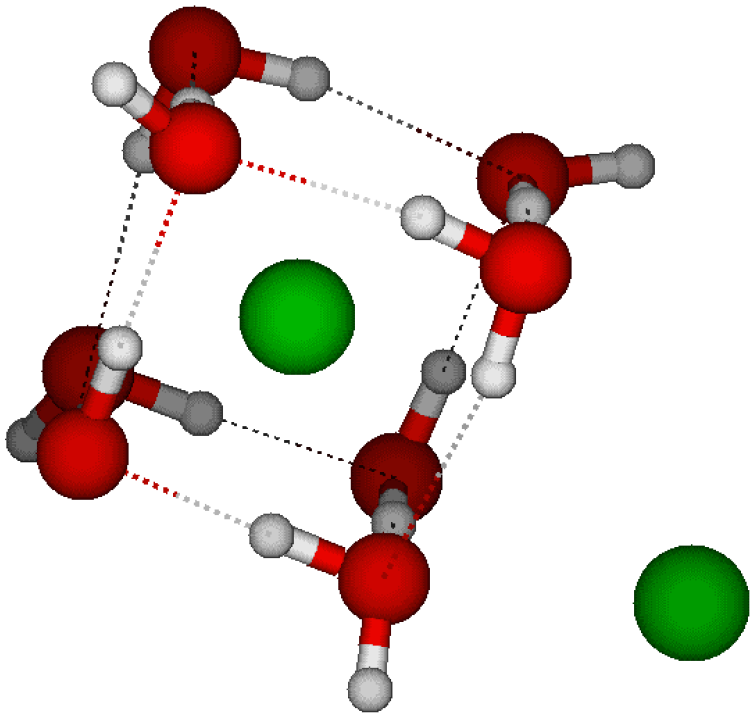

Figure 9.3. Structure of the 8-water, 1-electron system described in Example 9.2.

As indicated in Example 9.2, the electrons/holes need to be grouped at the top (or the bottom) of the geometry file, so that the non-electron/hole particles can be targeted with a single MOLCHARGE line (MOLCHARGE 3 26 0.00, Example 9.2) enabling normal charge transfer during reactions between the regular atoms.

Also, while electrons/holes can be put very close to the nuclei, they should not be put *exactly* on top of the atom – since this will results in a NaN results. However, even with a very small displacement from the atom (e.g. 0.001 Angstrom) the atom/electron/hole configuration will provide a meaningful result. As such – for building initial structures, when it is desired to put the electron/hole close to a particular atom it is advisable to copy the target atom location, rename the atom label to 'El' or 'Ho' for electron/holes, respectively, and then provide a small translation.

Control-file. Two control-keywords are of particular relevance for the e-ReaxFF method. First, and most important, the icharg-keyword (see Table 2.10) should be set to 7 to invoke the ACKS2 charge calculation method – which is essential to e-ReaxFF. Second, a new control-keyword, ielec, is available. Setting ielec=1 will create an additional trajectory output file (xmolout_el) in which the electrons or holes standard atom labels (El/Ho) are replaced with X – this enables direct visualization with Molden and VMD.

Force field file. A number of e-ReaxFF specific parameters are added to the ReaxFF force field file. Below is a list of these parameters and their general purpose. For a further explanation of the ACKS2 parameters, please see (Verstraelen et al., 2013)

General parameters (section 1 of the force field, see Example 2.8)
Parameter 27: Electron/hole repulsion (under development)
Parameter 35: ACSK2 softness parameter
Parameter 37: p_{val}, equation 9.3

Atom parameters (section 2 of the force field)
Parameter 13: p_{xel2}, equation 9.5
Parameter 23: ACKS2 softcut
Parameter 24: alfa, equation 9.2
Parameter 27: beta, equation 9.3

Bond parameters (section 3 of the force field)
Parameter 16: p_{xel1}, equation 9.5

10. Literature

Abolfath, R.M., van Duin, A.C.T., Biswas, P. and Brabec, T. (2011) Reactive Molecular Dynamics study on the first steps of DNA-damage by free hydroxyl radicals. Journal of Physical Chemistry A 115, 11045-11049.

Aktulga, H.M., Grama, A.Y., Pandit, S.A. and van Duin, A.C.T. (2012) REACTIVE MOLECULAR DYNAMICS: NUMERICAL METHODS AND ALGORITHMIC TECHNIQUES. SIAM Journal on Scientific Computing 34, C1-C23.

Aryanpour, M., van Duin, A.C.T. and Kubicki, J.D. (2010) Development of a Reactive Force Field for Iron-Oxyhydroxide Systems. Journal of Physical Chemistry A 114, 6298-6307.

Assowe, O., Politano, O., Vignal, V., Arnoux, P., Diawara, B., Verners, O. and van Duin, A.C.T. (2012) Reactive molecular dynamics simulation of the initial oxidation stages of Ni (111) in pure water: Effect of an applied electric field. Journal of Physical Chemistry 116, 11796-11805.

Bharati, A.K., Kamat, A.M. and van Duin, A.C.T. (2012) Study of effect of strain on the thermal conductivity of Zinc Oxide using the ReaxFF reactive force field. Computational and Theoretical Chemistry 987, 71-76.

Brenner, D.W. (1990) Empirical potential for hydrocarbons for use in simulating the chemical vapor deposition of diamond films. Physical Review B 42, 9458-9471.

Buehler, M.J., Tang, H., van Duin, A.C.T. and Goddard, W.A. (2007) Threshold crack speed controls dynamical fracture of silicon single crystals. Physical Review Letters 99, 165502/165501-165502/165504.

Buehler, M.J., van Duin, A.C.T. and Goddard, W.A. (2006) Multiparadigm modeling of dynamical crack propagation in silicon using a reactive force field. Physical Review Letters 96, 095505.

Castro-Marcano, F., Kamat, A.M., Russo, M.F., van Duin, A.C.T. and Mathews, J.P. (2012) Combustion of an Illinois No. 6 Coal Char Simulated Using an Atomistic Char Representation and the ReaxFF Reactive Force Field. Combustion and Flame 159, 1272-1285.

Chen, H.-P., Kalia, R.K., Kaxiras, E., Lu, G., Nakano, A., Nomura, K.-i., van Duin, A.C.T., Vashishta, P. and Yuan, Z. (2010) Embrittlement of Metal by Solute Segregation-Induced Amorphization. Physical Review Letters 104, 155502/155501-155502/155504.
Chenoweth, K., Cheung, S., van Duin, A.C.T., Goddard, W.A. and Kober, E.M. (2005) Simulations on the thermal decomposition of a poly(dimethylsiloxane) polymer using the ReaxFF reactive force field. Journal of the American Chemical Society 127, 7192-7202.
Chenoweth, K., van Duin, A.C.T., Dasgupta, S. and Goddard, W.A. (2009a) Initiation Mechanisms and Kinetics of Pyrolysis and Combustion of JP-10 Hydrocarbon Jet Fuel. Journal of Physical Chemistry A 113, 1740-1746.
Chenoweth, K., van Duin, A.C.T. and Goddard, W.A. (2008a) ReaxFF reactive force field for molecular dynamics simulations of hydrocarbon oxidation. Journal of Physical Chemistry A 112, 1040-1053.
Chenoweth, K., van Duin, A.C.T. and Goddard, W.A. (2009b) The ReaxFF Monte Carlo Reactive Dynamics Method for Predicting Atomistic Structures of Disordered Ceramics: Application to the Mo3VOx Catalyst. Angewandte Chemie-International Edition 48, 7630-7634.
Chenoweth, K., van Duin, A.C.T., Persson, P., Cheng, M.J., Oxgaard, J. and Goddard, W.A. (2008b) Development and application of a ReaxFF reactive force field for oxidative dehydrogenation on vanadium oxide catalysts. Journal of Physical Chemistry C 112, 14645-14654.
Fogarty, J.C., Aktulga, H.M., Grama, A.Y., van Duin, A.C.T. and Pandit, S.A. (2010) A reactive molecular dynamics simulation of the silica-water interface. Journal of Chemical Physics 132, 174704/174701-174704/174710.
Gale, J.D., Ratieri, P. and van Duin, A.C.T. (2011) A Reactive Force Field for Aqueous-Calcium Carbonate Systems. Phys. Chem. Chem. Phys. 13, 16666-16679.
Ganesh, P., Kent, P.R.C. and V., M. (2011) Formation, Characterization and Dynamics of Onion-like Carbon Structures from Nanodiamonds Using Reactive Force-Fields for Electrical Energy Storage. Journal of Applied Physics 110, 073506.
Goddard, W.A., III, Mueller, J.E., Chenoweth, K. and van Duin, A.C.T. (2010) ReaxFF Monte Carlo reactive dynamics: Application to resolving the partial occupations of the M1 phase of the MoVNbTeO catalyst. Catal. Today 157, 71-76.
Goken, E., Joshi, K., Russo, M., van Duin, A.C.T. and Castleman, A.W. (2011) The effect of formic acid addition on water cluster stability and structure. Journal of Physical Chemistry A 115, 4657-4664.
Huang, L., Bandosz, T., Joshi, K., van Duin, A.C.T. and Gubbins, K.E. (2013) Reactive adsorption of ammonia and ammonia/water on CuBTC metal-organic framework: a ReaxFF molecular dynamics simulation. Journal of Chemical Physics 138, 034102.
Islam, M., Kolesov, G., Verstraelen, T., Kaxiras, E. and van Duin, A.C.T. (2016) eReaxFF: A Pseudo-Classical Treatment of Explicit Electrons in ReaxFF Reactive Force Field Simulations. Journal of Chemical Theory and Computation 12, 3463-3472.
Islam, M. and van Duin, A.C.T. (2016) Reductive Decomposition Reactions of Ethylene Carbonate via Explicit Electrons: An eReaxFF Molecular Dynamics Study. Journal of Physical Chemistry 120, 27128-27134.
Jeon, B., Sankaranarayanan, S., van Duin, A.C.T. and Ramanathan, S. (2011) Atomistic insights into aqueous corrosion of copper. Journal of Chemical Physics 134, 234706-234701-234706-234709.

Jeon, B., Sankaranarayanan, S., van Duin, A.C.T. and Ramanathan, S. (2012) Reactive molecular dynamics study of chloride ion interaction with copper oxide surfaces in aqueous media. ACS Applied Materials and Interfaces 4, 1225-1232.
Jiang, D.E., van Duin, A.C.T., Goddard, W.A. and Dai, S. (2009) Simulating the Initial Stage of Phenolic Resin Carbonization via the ReaxFF Reactive Force Field. Journal of Physical Chemistry A 113, 6891-6894.
Joshi, K. and van Duin, A.C.T. (2013) Molecular dynamics study on the influence of additives on the high temperature structural and acidic properties of ZSM-5 zeolite. Energy and Fuels 27, 4481-4488.
Khalilov, U., Pourtois, G., Bogaerts, A., van Duin, A.C.T. and Neyts, E.C. (2013a) A new mechanism for oxidation of native silicon oxide. Journal of Physical Chemistry C 117, 9819-9825.
Khalilov, U., Pourtois, G., Bogaerts, A., van Duin, A.C.T. and Neyts, E.C. (2013b) Reactive Molecular Dynamics Simulations on SiO2-Coated Ultra-Small Si-Nanowires. Nanoscale 5, 719-725.
Khalilov, U., Pourtois, G., van Duin, A. and Neyts, E.C. (2012a) On the c-Si/a-SiO2Interface in Hyperthermal Si Oxidation at Room Temperature. Journal of Physical Chemistry C 116, 21856-21863.
Khalilov, U., Pourtois, G., van Duin, A.C.T. and Neyts, E.C. (2012b) Self-limiting Oxidation in Small Diameter Si Nanowires. Chemistry of Materials 24, 2141-2147.
Kim, S.-Y., Kumar, N., Persson, P., Sofo, J., van Duin, A.C.T. and Kubicki, J.D. (2012a) Development of a ReaxFF reactive force field for Titanium dioxide/water systems. Langmuir submitted.
Kim, S.-Y., van Duin, A.C.T. and Kubicki, J.D. (2012b) Simulations of the Interactions between TiO2 nanoparticles and Water with Na+ and Cl-, Methanol and Formic Acid Using a Reactive Force Field. Journal of Materials Research Accepted for publication.
Manzano, H., Pellenq, R., Ulm, F.-J., Buehler, M.J. and van Duin, A.C.T. (2012a) Hydration of calcium oxide predicted by reactive force field molecular dynamics. Langmuir 28, 4187-4197.
Manzano, H., Ulm, F.-J., van Duin, A., Pellenq, R., Marinelli, F. and Moeni, S. (2012b) Water polarization and dissociation in confined nanopores: mechanism, dipole distribution, and impact on the substrate properties. Journal of the American Chemical Society 134, 2208-2215.
Monti, S., Corozzi, A., Fristrup, P., Joshi, K., Shin, Y.K., Oelschlager, P., van Duin, A.C.T. and Barone, V. (2013) Exploring the conformational and reactive dynamics of biomolecules in solution using an extended version of the glycine reactive force field. Phys. Chem. Chem. Phys. 15, 15062-15077.
Monti, S., van Duin, A.C.T., Kim, S.-Y. and Barone, V. (2012) Exploration of the Conformational and Reactive Dynamics of Glycine During and After its Adsorption onto Titania: Computational Investigations in the Gas Phase and in Solution. Journal of Physical Chemistry C 116, 5141-5150.
Mortier, W.J., Ghosh, S.K. and Shankar, S. (1986) Electronegativity Equalization Method for the Calculation of Atomic Charges in Molecules. Journal of the American Chemical Society 108, 4315-4320.
Nakano, A., Kalia, R.K., Nomura, K., Sharma, A., Vashishta, P., Shimojo, F., van Duin, A.C.T., Goddard, W.A., Biswas, R. and Srivastava, D. (2007) A divide-and-

conquer/cellular-decomposition framework for million-to-billion atom simulations of chemical reactions. Computational Materials Science 38, 642-652.
Nakano, A., Kalia, R.K., Nomura, K.I., Sharma, A., Vashishta, P., Shimojo, F., Van Duin, A.C.T., Goddard, W.A., Biswas, R., Srivastava, D. and Yang, L.H. (2008) De novo ultrascale atomistic simulations on high-end parallel supercomputers. International Journal of High Performance Computing Applications 22, 113-128.
Neyts, E.C., Khalilov, U., Portois, G. and van Duin, A.C.T. (2011) Hyperthermal Oxygen Interacting with Silicon Surfaces: Adsorption, Implantation and Damage Creation. Journal of Physical Chemistry C 115, 4818-4823.
Neyts, E.C., van Duin, A.C.T. and Bogaerts, A. (2012) Insights in the Plasma Assisted Growth of Carbon Nanotubes through Atomic Scale Simulations: Effect of Electric Field. Journal of the American Chemical Society 134, 1256-1260.
Nomura, K., Kalia, R.K., Nakano, A., Vashishta, P. and van Duin, A.C.T. (2012) Mechanochemistry of Nanobubble Collapse near Silica in Water. Applied Physics Letters 101, 073108/073101-073108/073104.
Nomura, K.I., Kalia, R.K., Nakano, A., Vashishta, P., van Duin, A.C.T. and Goddard, W.A. (2007) Dynamic transition in the structure of an energetic crystal during chemical reactions at shock front prior to detonation. Physical Review Letters 99, 148303.
Pitman, M.C. and van Duin, A.C.T. (2012) Dynamics of Confined Reactive Water in Smectic Clay–Zeolite Composites. Journal of the American Chemical Society 134, 3042-3053.
Rahaman, O., van Duin, A.C.T., Bryantsev, V.S., Mueller, J.E., Solares, S.D., Goddard, W.A., III and Doren, D.J. (2010) Development of a ReaxFF Reactive Force Field for Aqueous Chloride and Copper Chloride. J. Phys. Chem. A 114, 3556-3568.
Rahaman, O., van Duin, A.C.T., Goddard, W.A., III and Doren, D.J. (2011) Development of a ReaxFF reactive force field for glycine and application to solvent effect and tautomerization. Journal of Physical Chemistry B 115, 249-261.
Raju, M., Fichthorn, K., Kim, S.-Y. and van Duin, A.C.T. (2013) ReaxFF Reactive Force Field Study of the Dissociation of Water on Titania Surfaces. Journal of Physical Chemistry C 117, 10558-10572.
Raymand, D., van Duin, A.C.T., Goddard, W.A., Hermansson, K. and Spangberg, D. (2011) Hydroxylation Structure and Proton Transfer Reactivity at the Zinc Oxide-Water Interface. Journal of Physical Chemistry A 115, 8573-8579.
Raymand, D., van Duin, A.C.T., Spangberg, D., Goddard, W.A. and Hermansson, K. (2010) Water adsorption on stepped ZnO surfaces from MD simulation. Surface Science 604, 741-752.
Russo, M., Li, R., Mench, M. and van Duin, A.C.T. (2011) Molecular Dynamic Simulation of Aluminum-Water Reactions Using the ReaxFF Reactive Force Field. International Journal of Hydrogen Energy 36, 5828-5835.
Salmon, E., van Duin, A.C.T., Lorant, F., Marquaire, P.M. and Goddard, W.A. (2009a) Early maturation processes in coal. Part 2: Reactive dynamics simulations using the ReaxFF reactive force field on Morwell Brown coal structures. Organic Geochemistry 40, 1195-1209.
Salmon, E., van Duin, A.C.T., Lorant, F., Marquaire, P.M. and Goddard, W.A. (2009b) Thermal decomposition process in algaenan of Botryococcus braunii race L. Part 2:

Molecular dynamics simulations using the ReaxFF reactive force field. Organic Geochemistry 40, 416-427.
Senftle, T., Hong, S., Islam, M., Kylasa, S.B., Zheng, Y., Shin, Y.K., Junkermeier, C., Engel-Herbert, R., Janik, M., Aktulga, H.M., Verstraelen, T., Grama, A.Y. and van Duin, A.C.T. (2016) The ReaxFF Reactive Force-field: Development, Applications, and Future Directions. Nature Computational Materials 2, 15011.
Shan, T.-R., Wixom, R.R., Mattson, A.E. and Thompson, A.P. (2013) Atomistic Simulation of Orientation Dependence in Shock-Induced Initiation of Pentaerythritol Tetranitrate. Journa of Physical Chemistry B 117, 928-936.
Srinivasan, S.G. and van Duin, A.C.T. (2011) A molecular dynamics based study of the collisions of hyperthermal atomic oxygen with graphene using the ReaxFF reactive force field. Journal of Physical Chemistry A 115, 13269-13280.
van Duin, A.C.T., Bryantsev, V.S., Diallo, M.S., Goddard, W.A., Rahaman, O., Doren, D.J., Raymand, D. and Hermansson, K. (2010) Development and validation of a ReaxFF reactive force field for Cu cation/water interactions and copper metal/metal oxide/metal hydroxide condensed phases. Journal of Physical Chemistry A 114, 9507-9514.
van Duin, A.C.T., Dasgupta, S., Lorant, F. and Goddard, W.A. (2001) ReaxFF: A reactive force field for hydrocarbons. Journal of Physical Chemistry A 105, 9396-9409.
van Duin, A.C.T., Zou, C., Joshi, K., Bryantsev, V.S. and Goddard, W.A. (2012) A ReaxFF reactive force field for proton transfer reactions in bulk water and its applications to heterogeneous catalysis.
Vashishta, P., Kalia, R.J. and Nakano, A. (2006) Multimillion Atom Simulations of Dynamics of Oxidation of an Aluminum Nanoparticle and Nanoindentation on Ceramics. Journal of Physical Chemistry B 110, 3727-3733.
Vedadi, M., Choubey, A., Nomura, K., Kalia, R.K., Nakano, A., Vashishta, P. and van Duin, A.C.T. (2010) Structure and Dynamics of Shock-Induced Nanobubble Collapse in Water. Physical Review Letters 105, 014503/014501-014503/014504.
Verstraelen, T., Ayers, P.W., Van Speybroeck, V. and Waroquier, M. (2013) ACKS2: atom-condensed Kohn-Sham DFT approximated to second order. Journal of Chemical Physics 138, 074108.
Yusupov, M., Khalilov, U., Neyts, E.C., Snoeckx, R., van Duin, A.C.T. and Bogaerts, A. (2012) Atomic scale simulations of plasma species interacting with bacteria cell walls. New Journal of Physics 14, 093043.
Zou, C., van Duin, A.C.T. and Sorescu, D. (2012) Theoretical investigation of hydrogen adsorption and dissociation on iron and iron carbide surfaces using the ReaxFF reactive force field method. Topics in Catalysis 55, 391-401.
Zybin, S.V., Goddard, W.A., III, Xu, P., van Duin, A.C.T. and Thompson, A.P. (2010) Physical mechanism of anisotropic sensitivity in pentaerythritol tetranitrate from compressive-shear reaction dynamics simulations. Applied Physics Letters 96, 081918/081911-081918/081913.